Article

Temperature-Related N₂O Emission and Emission Potential of Freshwater Sediment

Shuai Li [1,†], Ang Yue [2,3,†], Selina Sterup Moore [4], Fei Ye [1], Jiapeng Wu [1], Yiguo Hong [1] and Yu Wang [1,*]

[1] Key Laboratory for Water Quality and Conservation of the Pearl River Delta, Ministry of Education, Institute of Environmental Research at Greater Bay, Guangzhou University, Guangzhou 510006, China
[2] School of Environmental Science and Engineering, Tianjin University, Tianjin 300350, China
[3] Tianjin Eco-Environmental Monitoring Center, Tianjin 300191, China
[4] Department of Agronomy, Food, Natural Resources, Animals and Environment (DAFNAE), University of Padova, 35122 Padova, Italy
[*] Correspondence: wangyu@gzhu.edu.cn
[†] These authors contributed equally to this work.

Abstract: Nitrous oxide (N₂O) is a major radiative forcing and stratospheric ozone-depleting gas. Among natural sources, freshwater ecosystems are significant contributors to N₂O. Although temperature is a key factor determining the N₂O emissions, the respective effects of temperature on emitted and dissolved N₂O in the water column of freshwater ecosystems remain unclear. In this study, 48 h incubation experiments were performed at three different temperatures; 15 °C, 25 °C, and 35 °C. For each sample, N₂O emission, dissolved N₂O in the overlying water and denitrification rates were measured, and N₂O-related functional genes were quantified at regular intervals. The highest N₂O emission was observed at an incubation of 35 °C, which was 1.5 to 2.1 factors higher than samples incubated at 25 °C and 15 °C. However, the highest level of dissolved N₂O and estimated exchange flux of N₂O were both observed at 25 °C and were both approximately 2 factors higher than those at 35 °C and 15 °C. The denitrification rates increased significantly during the incubation period, and samples at 25 °C and 35 °C exhibited much greater rates than those at 15 °C, which is in agreement with the N₂O emission of the three incubation temperatures. The NO_3^- decreased in relation to the increase of N₂O emissions, which confirms the dominant role of denitrification in N₂O generation. Indeed, the *nirK* type denitrifier, which constitutes part of the denitrification process, dominated the *nirS* type involved in N₂O generation, and the *nosZ* II type N₂O reducer was more abundant than *the nosZ* I type. The results of the current study indicate that higher temperatures (35 °C) result in higher N₂O emissions, but incubation at moderate temperatures (25 °C) causes higher levels of dissolved N₂O, which represent a potential source of N₂O emissions from freshwater ecosystems.

Keywords: freshwater lake; N₂O emission; dissolved N₂O; temperature sensitivity

1. Introduction

Nitrous oxide (N₂O) constitutes a significant source of global greenhouse gases [1,2], and it plays a major role in ozone depletion in the stratosphere [3]. Therefore, knowledge of the production and emission of N₂O is of great use for scientists to further understand the processes of global warming and the destruction of the stratospheric ozone layer [4]. N₂O is produced by multiple biological pathways, including nitrification, denitrification, and dissimilatory nitrate reduction to ammonium [5,6]. Nitrification is generally the main N₂O source under oxic conditions in soil [7], while denitrification is the main source in the anaerobic environment [8]. Due to different irrigation patterns, such as alternate wetting and drying (AWD) and continuous flooding (CF), the c showed diverse results. In AWD irrigation, the peak of N₂O emission occurred both during the dry and c period. While the emission peak occurred only after fertilizer application in CF conditions. [9]. Because of the aerobic and anaerobic alternation provided by AWD irrigation, nitrification

and denitrification were enhanced. The substrate for microbial activity was provided by fertilization. Both of them made a high N_2O emission. However, the continuously anaerobic condition of CF was not favorable for N_2O emission [10]. Because of the high content of organic matter and the anaerobic environment of the sediment [11], the N_2O emissions in aquatic systems are generally much greater than those in soil. This is the result of denitrification processes which greatly dominate over nitrification processes in the generation of N_2O.

Freshwater ecosystems currently produce about 1.8 Tg N-N_2O per year and account for about 25% of global N_2O emissions [12]. The N_2O emissions from freshwater ecosystems are influenced by a variety of environmental factors, such as temperature, pH, dissolved oxygen (DO) and nitrogen concentration in the sediment [13–15]. Among them, temperature has been demonstrated to greatly influence N_2O emissions [16,17]. Most studies suggest that higher temperatures increase microbial activity, which leads to increased N_2O release. For example, the N_2O emissions in aquatic ecosystems are normally higher in summer than in colder periods of the year [18,19]. Additionally, freshwater lakes with similar annual temperatures have been shown to have comparable N_2O emission rates, while these rates were higher for lakes exposed to lower temperatures [20]. With the recent findings concerning N_2O-reducing processes and microorganisms, the quest to elucidate the ways by which N_2O emissions are affected has become ever more complicated [21]. It has been observed that increased temperatures promote the greater activity of specific microbes able to reduce N_2O to N_2, thereby decreasing N_2O emissions [22]. On the contrary, a study has reported that N_2O emissions do not respond to variations in temperature [23]. These inconsistent results on the relation between temperature and N_2O emissions could be ascribed to the complicated environmental factors in situ conditions, differing methodologies, such as differences in N_2O gas collection, or the fact that the dominant microbial process of N_2O generation and reduction varied in the studied habitats [24].

To identify the relationship between temperature and N_2O emissions, sediment samples from a freshwater lake located in Guangzhou, China, were collected for incubation experiments at three different temperatures; 15 °C, 25 °C and 35 °C. It was hypothesized that the high N_2O might occur at a higher temperature because of the high microbial activity. Both N_2O emissions and the level of dissolved N_2O in the water column were collected in a time series. By measuring the N_2O concentration, denitrification activity and N_2O-related gene abundance, the current study aims to (i) show the response of N_2O emissions and dissolved N_2O to different temperatures; and (ii) elucidate the microbial background underlying these variations in N_2O characteristics.

2. Materials and Methods

2.1. Experimental Set Up

Sediment and overlying water material were collected in parallel in May 2022 at a waterbody in Guangzhou, China, to be used for incubation experiments which lasted for 48 h. The annual mean temperature at the site ranges between 18–26 °C. The sediment material was incubated in 10 L incubators (POMEX, Beijing, China), and the collected overlying water was hereafter added to a ratio of 3:4 (*v/v*). The incubations were run at ambient temperatures of 15 °C, 25 °C, and 35 °C controlled by the temperature-controlled incubators. The first sediment and water samples with three replications were taken 12 h after the onset of the incubation experiment to allow ample time for the microbes to acclimatize to the new temperature. Thereafter, sampling took place in 4 h intervals until the 36 h. A final sampling was made at the 48 h.

2.2. Physicochemical Analysis

Sediment ammonium (NH_4^+), nitrite (NO_2^-), and nitrate (NO_3^-) were extracted from 2 g of fresh sediment with 10 mL of 2 M KCl (1:5 wt./vol). The supernatant was filtered through a 0.22 μm membrane filter (Jinlong, Tianjin, China) and determined via a spectrophotometric detection assay [25].

2.3. Calculating N_2O Exchange Flux

The gas exchange flux at the water-gas interface is calculated using the following equation based on the dissolved N_2O:

$$F = k \times (C_{obs} - C_{eq}) \tag{1}$$

where F (nmol/m^2·h) is the water-air exchange flux. k (cm·h^{-1}) is the gas exchange rate. C_{obs} is the measured concentration of dissolved N_2O as mentioned above, and C_{eq} (nmol·L^{-1}) is the concentration of N_2O in the surface water at equilibrium with the atmosphere, which can be calculated using the following equation [26]:

$$LnF = A_1 + A_2(100/T) + A_3 \times Ln(T/100) + A_4 \times (T/100)^2 + S \times \left[B_1 + B_2 \times (T/100) + B_3 \times (T/100)^2\right]$$

$$C_{eq} = F \times C_{N_2O \text{ in atmosphere}} \times 10^9 \tag{2}$$

where F is experiment value in (mol/L·atm), A_1 = −165.8806, A_2 = 222.8743, A_3 = 92.0792, A_4 = −1.48425, B_1 = −0.056235, B_2 = 0.031619, B_3 = −0.0048472. It is assumed that the concentration of N_2O in the atmosphere is 325×10^{-9}.

The gas exchange rate k (cm·h^{-1}) is measured by the gas tracer method according to the Wanninkhof formula model can accurately estimate the gas exchange rate at different wind speeds [27].

$$k = 0.31 \times U_{10}^2 \times \left(\frac{S_c}{660}\right)^{\frac{1}{2}} \tag{3}$$

where U_{10} is the wind speed in m·s^{-1} at the height of 10 m above the water surface, this paper uses the short-term wind speed data corresponding to the sampling moment. Sc number is the ratio of the dynamic viscosity of water to the diffusion rate of the gas molecules to be measured. Wanninkhof (1992) gives the relationship between the Sc number of N_2O gas and the water temperature:

$$Sc_{N_2O} = 2055.6 - 137.11 \times T + 4.3173 \times T^2 - 0.05435 \times T^3 \tag{4}$$

where T is the water temperature.

2.4. Measurements of N_2O Emission and Dissolved N_2O

Both the emitted N_2O in the containers and the dissolved N_2O in the overlying water were measured. The emitted N_2O was determined by directly extracting gas samples from the headspace of each incubation experiment at 0 h, 12 h, 16 h, 20 h, 24 h, 36 h, 40 h, 44 h and 48 h [28]. The dissolved N_2O was determined by headspace equilibrium-gas chromatography [29]: briefly, the water sample was filled into 60 mL serum bottles, and 1 mL of 50% $ZnCl_2$ was added to inhibit the microbial activity [30]. 10 mL helium gas was injected into the serum bottles to act as a replacement for the water sample in order to create a headspace. The sample bottle was shaken vigorously for 30 min to equilibrate the gas-liquid phase in the bottle. After resting for 30 min to 1 h, the headspace volume was injected into the gas chromatograph for determination [31]. The concentration of N_2O was measured with a gas chromatograph (GC-2014C, Shimadzu, Japan) equipped with an electron capture detector (ECD).

2.5. Measurement of Denitrification Rate in Sediment

The denitrification rate of the sediment samples was measured at 0 h, 24 h and 48 h at the set temperatures using the slurry incubation and isotope pairing technique [32]. Fresh sediments were mixed with water in the ratio of 1:7 (sediment: water) and flushed with ultrahigh purity He for 30 min to promote the development of anaerobic sediment slurries. These slurries were pre-incubated in the dark at the set temperature for 36–48 h to remove

background NO_x^- (NO_3^- and NO_2^-) and dissolved oxygen (DO). After pre-incubation, the slurries were transferred to 12.5 mL tubes (Exetainers, Labco, High Wycombe, UK) via injectors. These tubes were divided into two groups: the first group was used to analyze F_n ($^{15}NO_3^-/NO_x^-$), and the second was injected with a $^{15}NO_3^-$ (99.6 atom%) solution to a final concentration of 100 μM. The tubes were incubated in the incubator (POMEX, Beijing, China) at the corresponding temperature, and microbial activity was stopped by adding 0.5 mL of 50% ($v{:}v$ = 1:1) $ZnCl_2$ at 0 h and 2 h from the beginning of incubation. The $^{29}N_2$ and $^{30}N_2$ produced in the tubes were determined with a membrane inlet mass spectrometry (MIMS, HPR40, Hiden, UK), and the rates of denitrification were calculated as follows [33]:

$$R_D = D_{29} + 2 \times P_{30} D_{29} = P_{30} \times 2 \times (1 - F_n) \times F_n^{-1} \tag{5}$$

where R_D (nmol N g^{-1} h^{-1}) represented the total rate of $^{15}NO_3^-$—based denitrification, D_{29} was the $^{29}N_2$ production rate from denitrification, P_{30} (nmol N g^{-1} h^{-1}) was the total $^{30}N_2$ production rate; F_n represented the fraction of ^{15}N in total NO_3^-.

The N_2O saturation was calculated based on the actual concentration of dissolved N_2O and the saturated concentration of N_2O at corresponding temperatures.

$$\sigma = (C - C_0)/C_0 \tag{6}$$

where C (nmol/L) represents the actual concentration of dissolved N_2O, C_0 is the saturated concentration of N_2O at gas-liquid equilibrium.

2.6. Statistical Analysis

To test significant differences between samples, one-way analysis of variance (ANOVA) was used for the normally distributed variables. The Pearson correlation or nonparametric Spearman correlation coefficients were then calculated to examine the relationship between samples. A significance level of $p < 0.05$ was used for all statistical analyses, which were carried out using the SPSS 22.0 software platform (SPSS Inc. Chicago, IL, USA).

Further explanation of DNA extraction, sequencing, and quantitative PCR (Table S1) can be found in the Supplementary Materials.

3. Results

3.1. N₂O Emission and Dissolved N₂O

During the 48 h incubation, higher levels of N_2O emission were observed at 35 °C (2.3 mmol N_2O/g soil average), which was higher than that at 25 °C (1.7 mmol N_2O/g soil average) and 15 °C (1.6 mmol N_2O/g soil average). The highest N_2O emission at 25 °C and 35 °C both occurred at 16 h, which were 2.3 and 3.5 mmol N_2O/g soil, respectively. At 15 °C, the highest N_2O emission was found at 36 h. After 36 h, the N_2O emissions were similar across all three temperatures, and all had a downward tendency (Figure 1a).

The dissolved N_2O showed a different pattern to the N_2O emission (Figure 1b); the average dissolved N_2O at 25 °C (140.9 nmol/L) was considerably higher than those at 35 °C (74.2 nmol/L) and 15 °C (70.6 nmol/L). The highest concentrations at 25 °C occurred between 12 h and 20 h, with concentrations around 215.9 and 250.3 nmol/L. The dissolved N_2O at 15 °C and 35 °C were low and similar to each other at an average of 70.6 and 74.2 nmol/L, respectively. Furthermore, the dissolved N_2O after 36 h was similar across the three temperatures.
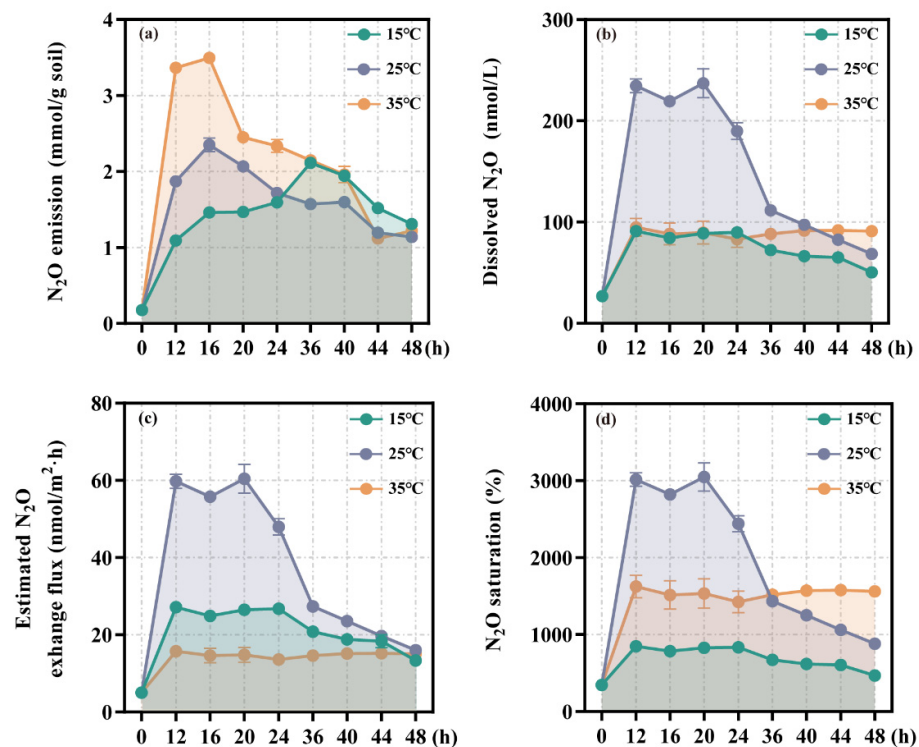
Figure 1. N_2O emission (**a**), dissolved N_2O (**b**), estimated N_2O exchange flux (**c**) and N_2O saturation (**d**) at incubations of 15 °C, 25 °C and 35 °C.

The estimated N_2O exchange flux was greatest at 25 °C with an average flux of 35.1 nmol/m²·h, which was significantly higher than that at 15 °C (ANOVA, $p = 0.085$) and 35 °C (ANOVA, $p = 0.006$). Incubation at 35 °C demonstrated the lowest estimated N_2O exchange flux at 13.8 nmol/m²·h (Figure 1c, Table S2). The N_2O saturation was highest between 12 h and 20 h at 25 °C, ranging between 2820.3% and 3038.3% (Figure 1d). Although the dissolved concentrations were lower at 15 °C and 35 °C, they were nonetheless saturated at 785.2–847.5% and 1515.5–1626.6%, respectively.

3.2. Denitrification Rate in Sediment and the Concentration of Inorganic Nitrogen in Water

Higher mean denitrification rates in sediment were observed at 25 °C and 35 °C (12.5 and 12.8 nmol/g·h) than that at 15 °C (8.2 nmol/g·h). The denitrification rates increased significantly with incubation time, in which higher rates were observed at 24 h than at 0 h in all three temperatures (ANOVA, $p = 0.031$, 0.057 and 0.025, respectively). The denitrification rate at 48 h was also higher than that at 24 h at 25 °C. The anammox rates were lower than the denitrification rates and showed minor variation with the denitrification rates (Figure 2a–c).

The increase in the denitrification rate was in accordance with the decrease in NO_3^- concentration. Clear decreases in NO_3^- from 27.4 to 6.5 µmol/L and 27.4 to 0 µmol/L were observed at 25 °C and 35 °C, respectively (Figure 2d). NO_2^- was detected at a relatively low concentration in the overlying water at 35 °C with an increase from 2.4 to 3.9 µmol/L (Figure 2e). The NH_4^+ content of the overlying water increased from 0 to 6.1 µmol/L at 15 °C, 0 to 12.8 µmol/L at 25 °C and 0 to 22.2 µmol/L at 35 °C before the 15 h, respectively. No clear trend was observed after 20 h of incubation (Figure 2f).
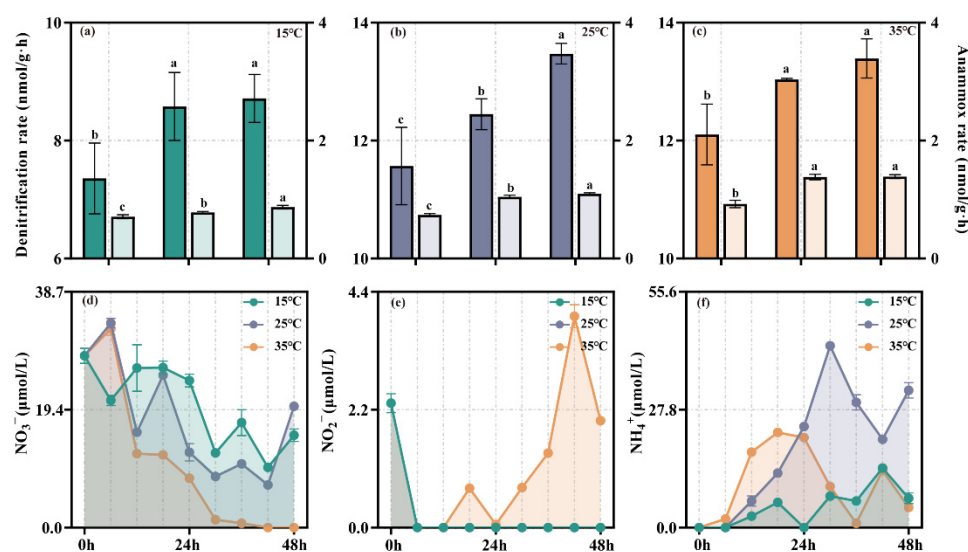
Figure 2. Denitrification and anammox rates at hours 0, 24 and 48 in 15 °C (**a**), 25 °C (**b**) and 35 °C (**c**). The concentration of NO_3^- (**d**), NO_2^- (**e**) and NH_4^+ (**f**) in the overlying water during incubation at 15, 25 and 35 °C. The a, b and c above the columns were the results tested by ANOVA. Different letters indicate significant differences among treatments ($p < 0.05$).

3.3. Abundance of N₂O-Related Functional Gene in Sediment

The abundance of functional genes related to denitrification (*nirK*, *nirS*, *nosZ* I and *nosZ* II) kept relatively stable and had no obvious trend over time (Figure S1). The abundance of the *nirK* gene varied from 3.43×10^8 to 1.42×10^9 copies/g dry soil, which was 1 order of magnitude higher than that of *nirS*. There was no significant difference in *nirK* gene abundance among the three temperatures. The abundance of *the nirS* gene was significantly higher (ANOVA, $p = 0$) at 15 °C (2.97×10^8 copies/g dry soil) than at 25 °C (2.49×10^8 copies/g dry soil) and 35 °C (2.41×10^8 copies/g dry soil) (Figure 3a). The abundance of the *nosZ* II gene was 1 order of magnitude higher than *nosZ* I. The abundance of *the nosZ* II gene was significantly higher (ANOVA, $p = 0.005$) at 15 °C (1.55×10^8 copies/g dry soil) than at 25 °C (1.34×10^8 copies/g dry soil) and 35 °C (1.33×10^8 copies/g dry soil) (Figure 3b). The gene abundance *nirS* + *nirK* was 5 to 10 times higher than that of *nosZ* I + *nosZ* II, and there was no significant difference among the ratio of *nirS* + *nirK*/*nosZ* I + *nosZ* II at the three incubation temperatures (Figure 3c).
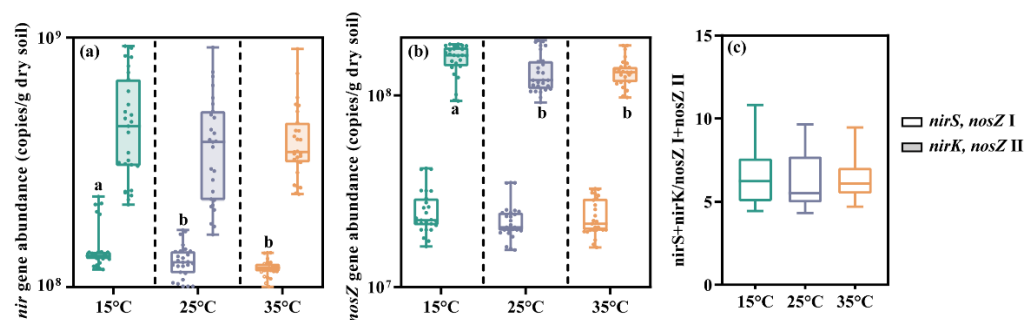

Figure 3. The abundance of N₂O-related functional genes (*nirS*, *nirK*) (**a**), and (*nosZ* I, *nosZ* II) (**b**) at different temperatures and the ratio of (*nirS* + *nirK*)/(*nosZ* I + *nosZ* II) (**c**). (The a, b and c above the columns were the results tested by ANOVA. Different letters indicate significant differences among treatments ($p < 0.05$).

3.4. Factors Determining the N₂O Generation

At 15 °C, the dissolved N₂O and N₂O emissions were mainly related to the NO_3^- (Figure S2, Table S3). The dissolved N₂O in the overlying water increased from 66.4 nmol/L

to 91.1 nmol/L, along with higher NO_3^- content (Figure 4a). At 25 °C, the dissolved N_2O, N_2O emission and the derived ratio parameters were mainly related to the ratio of *nirS*/*nirK* and *nosZ* I/*nosZ* II. Especially, the dissolved N_2O in the overlying water had a positive correlation with the ratio of *nirS*/*nirK* ($p < 0.05$) (Figure 4b). At 35 °C, the dissolved N_2O, N_2O emission and the derived ratios were mainly related to NO_3^-, NO_2^-, NO_3^-/DIN and NO_2^-/DIN. N_2O emission was positively correlated with the NO_3^- ($p < 0.05$) that the N_2O emission increased from 1.1 mmol N_2O/g soil to 3.5 mmol N_2O/g soil as the NO_3^- increased from 0 mg/L to 2 mg/L (Figure 4c).
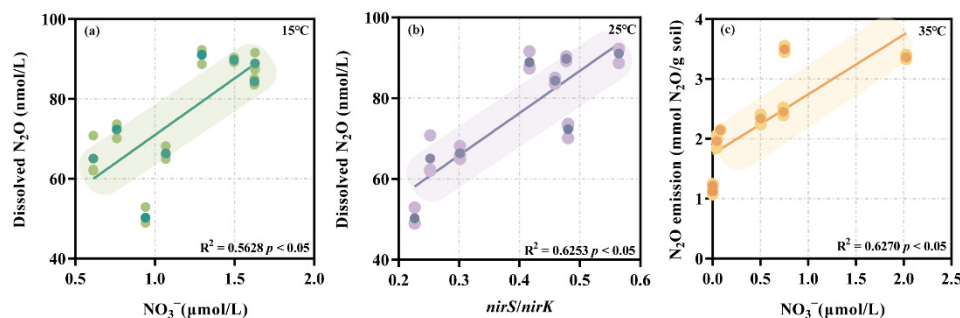

Figure 4. Correlation of the dissolved N_2O and NO_3^- at 15 °C (**a**), dissolved N_2O and *nirS*/*nirK* ratio at 25 °C (**b**), N_2O emission and NO_3^- at 35 °C (**c**). Dark points represent the mean values for each sampling time during 48-incubation, and light points represent all survey data.

4. Discussion

In this study, the average N_2O emission at 35 °C was 1.5 to 2.1 times higher than that at 25 °C and 15 °C, suggesting that the N_2O generation was temperature sensitive in freshwater sediment. This is in accordance with previous studies [34,35].

For example, the N_2O emissions were nearly 36 times higher in summer than in winter in polar freshwater lakes, which was ascribed to the enhanced rate of coupled nitrification-denitrification in summer [34]. Similarly, N_2O emissions were 2 times higher at 25 °C than that at 15 °C in soil, in which the faster growth of the microbial community induced a higher N_2O emission at higher temperatures [35]. Likewise, the N_2O emission was found to be more sensitive to temperature in wastewater treatment plants: the N_2O released from the water-gas interface was about three times higher at 35 °C than that at 25 °C, and the denitrification rate accordingly increased by 62% when the temperature increased from 25 °C to 35 °C [36]. Hence, higher temperatures directly increased the activity of denitrification as well as the N_2O emission [37,38]. Moreover, the increased temperatures could enhance N_2O emission by decreasing the organic carbon, thereby increasing the likelihood of incomplete denitrification and, therefore, also the likelihood for N_2O to be produced as an intermediate product [39].

It was noted that the highest saturation and estimated exchange flux of N_2O were observed at 25 °C, which were both about 2 times higher than those at 35 °C and 15 °C. The dissolved N_2O was in a state of oversaturation (667.3%, 1811.2% and 1408.4% at 15 °C, 25 °C and 35 °C, respectively) in all samples, suggesting that N_2O had a high potential for being released into the atmosphere. The saturation of N_2O in the current study was higher than those reported from natural habitats, including freshwater reservoirs, rivers and estuaries, with a saturation of 84% to 745%, 152–451% and 45–2187%, respectively [40,41]. This could be due to the relatively stable and inert environmental conditions in the incubation, allowing for the accumulation of N_2O in water. The microbial activity and the solubility of N_2O in the water were two key factors determining the dissolved N_2O in in situ conditions. Higher temperatures stimulated microbial activity and generated more N_2O [35] but decreased the solubility of N_2O in water [42]. Henry's constant, which is also called the air-water partition coefficient, rested on the temperature condition [43]. Henry's constant of N_2O in water increased from 4146 k_H/Pa·m^3·mol^{-1} to 6010 k_H/Pa·m^3·mol^{-1} when the temperature increased from 25 °C to 40 °C [43]. Theoretically, the N_2O solubility in pure

water decreased by 23% when the temperature increased from 25 °C to 35 °C [44]. In a field survey, the N_2O solubility was 125–385% less than in the current ex-situ study, which can be attributed to more N_2O being diffused into the headspace and the slower re-dissolution of N_2O caused by higher accumulation in the gas phase at higher temperature [36]. However, it is important to note the dissolved N_2O merely suggests a potential for emission and not an actual emission per se. The N_2O in water still had a great probability of being reduced by microorganisms carrying the *nosZ* gene before being emitted into the atmosphere [21].

The increase in temperature might influence many other factors such as soil organic carbon, nutrient availability and mineralization rate, etc. For example, the temperature sensitivity of soil organic carbon is lower in subtropical forests but higher in temperate forests. The C:N ratio of soil is significantly and positively correlated with organic carbon temperature sensitivity [45].

In this study, there was a significant increase in denitrification rates over time, and a positive correlation was observed between the denitrification rate and N_2O emission at the three temperatures, which indicated that the denitrification processes might dominate the N_2O emission. This is in accordance with previous studies in freshwater [46], tidal wetlands [47], riparian zones [48] and urban rivers [49], where the higher denitrification rates corresponded to higher N_2O fluxes. In addition, the habitats in which denitrification dominates the N_2O emission are usually sinks for NO_3^- [48]. It has previously been observed that the NO_3^- content shows a strong correlation with the N_2O emission in many habitats, including deep wells [50], freshwater rivers and lakes, etc. [51,52], and indeed, the NO_3^- content has been used as an indicator for the N_2O emission [53]. In this study, the NO_3^- showed a sharp decline, especially at high temperatures, presenting a negative relationship with the N_2O emission, which confirmed the dominant role of denitrification in N_2O emission. However, it cannot be ruled out that the DNRA pathway does not play a role since an increase of NH_4^+ was concurrently observed. In the present study, the total *nir/nos* ratio was between 5 and 10, indicating that the microbial community had a higher potential to produce N_2O than to reduce it [52,54]. It was confirmed by the high ratio of *nirK* to *nirS*, which was 1.2 to 2.4, that *nirK*-type denitrifies are more likely to perform incomplete denitrification and thereby contribute more to N_2O emissions [21].

5. Conclusions

The present study showed that the highest N_2O emission in freshwater sediment is observed at an elevated temperature of 35 °C. This was demonstrated through a series of incubation experiments with a temperature gradient at 15 °C, 25 °C and 35 °C. In contrast, the dissolved N_2O in the water column had a different pattern than that of N_2O emission; the highest concentration was namely observed at 25 °C, indicating that the highest potential of N_2O emission occurs at moderate temperatures. The denitrification rates significantly increased during incubation, while the rates at 25 °C and 35 °C were much greater than that at 15 °C, which coincides with the N_2O emissions at the three temperatures. The NO_3^- content was a key indicator of denitrification, which decreased along with the increase in N_2O emissions, thereby presenting a negative relationship between them. The *nirK*-type denitrifier dominated denitrification and N_2O generation, while the *nosZ* II-type denitrifier dominated N_2O reduction. The current analysis indicates that high temperatures (35 °C) may enhance denitrification-derived N_2O emissions, and moderated temperatures (25 °C) have higher dissolved N_2O, making it a potential source of N_2O emissions from freshwater ecosystems.

Table S3: The estimated N$_2$O exchange flux at three different temperatures. References [55–58] are listed in Supplementary Materials.

References

1. Neubauer, S.C.; Megonigal, J.P. Moving Beyond Global Warming Potentials to Quantify the Climatic Role of Ecosystems. *Ecosystems* **2015**, *18*, 1000–1013. [CrossRef]
2. Seitzinger, S.P.; Styles, R.V.; Kroeze, C. Global distribution of N$_2$O emissions from aquatic systems: Natural emissions and anthropogenic effects. *Chemosphere Glob. Chang. Sci.* **2000**, *2*, 267–279. [CrossRef]
3. Ravishankara, A.R.; Daniel, J.S.; Portmann, R.W. Nitrous oxide (N$_2$O): The dominant ozone-depleting substance emitted in the 21st century. *Science* **2009**, *326*, 123–125. [CrossRef]
4. Crutzen, P.J. The influence of nitrogen oxides on the atmospheric ozone content. *Q. J. R. Meteorol. Soc.* **1970**, *96*, 320–325. [CrossRef]
5. Rütting, T.; Boeckx, P.; Müller, C.; Klemedtsson, L. Assessment of the importance of dissimilatory nitrate reduction to ammonium for the terrestrial nitrogen cycle. *Biogeosciences* **2011**, *8*, 1779–1791. [CrossRef]
6. Wrage, N.; Velthof, G.L.; Beusichem, M.; Oenema, O. Role of nitrifier denitrification in the production of nitrous oxide. *Soil Biol. Biochem.* **2001**, *33*, 1723–1732. [CrossRef]
7. Skiba, U.; Smith, K.A. Nitrification and denitrification as sources of nitric oxide and nitrous oxide in a sandy loam soil. *Soil Biol. Biochem.* **1993**, *25*, 1527–1536. [CrossRef]
8. Bradley, R.L.; Whalen, J.; Chagnon, P.L.; Lanoix, M.; Alves, M.C. Nitrous oxide production and potential denitrification in soils from riparian buffer strips: Influence of earthworms and plant litter. *Appl. Soil Ecol.* **2011**, *47*, 6–13. [CrossRef]
9. Islam, S.M.M.; Gaihre, Y.K.; Islam, M.R.; Khatun, A.; Islam, A. Integrated Plant Nutrient Systems Improve Rice Yields without Affecting Greenhouse Gas Emissions from Lowland Rice Cultivation. *Sustainability* **2022**, *14*, 11338. [CrossRef]
10. Islam, S.M.M.; Gaihre, Y.K.; Islam, M.R.; Ahmed, M.N.; Akter, M.; Singh, U.; Sander, B.O. Mitigating greenhouse gas emissions from irrigated rice cultivation through improved fertilizer and water management. *J. Environ. Manag.* **2022**, *307*, 114520. [CrossRef]
11. Vilain, G.; Garnier, J.; Decuq, C.; Lugnot, M. Nitrous oxide production from soil experiments: Denitrification prevails over nitrification. *Nutr. Cycl. Agroecosystems* **2014**, *98*, 169–186. [CrossRef]
12. Seitzinger, S.P.; Kroeze, C. Global distribution of nitrous oxide production and N inputs in freshwater and coastal marine ecosystems. *Glob. Biogeochem. Cycles* **1998**, *12*, 93–113. [CrossRef]
13. De Klein, C.A.M.; Sherlock, R.R.; Cameron, K.C.; Van der Weerden, T.J. Nitrous oxide emissions from agricultural soils in New Zealand—A review of current knowledge and directions for future research. *J. R. Soc. N. Z.* **2001**, *31*, 543–574. [CrossRef]
14. Saggar, S.; Jha, N.; Deslippe, J.; Bolan, N.S.; Luo, J.; Giltrap, D.L.; Kim, D.G.; Zaman, M.; Tillman, R.W. Denitrification and N$_2$O:N$_2$ production in temperate grasslands: Processes, measurements, modelling and mitigating negative impacts. *Sci. Total Environ.* **2013**, *465*, 173–195. [CrossRef] [PubMed]
15. Wu, L.; Rees, R.M.; Tarsitano, D.; Zhan, X.; Jone, S.K.; Whitmor, A.P. Simulation of nitrous oxide emissions at field scale using the SPACSYS model. *Sci. Total Environ.* **2015**, *530*, 76–86. [CrossRef] [PubMed]
16. Mosier, A.R. Nitrous oxide emissions from agricultural soils. *Fert. Res.* **1994**, *37*, 191–200. [CrossRef]
17. Abdalla, M.; Smith, P.; Williams, M. Emissions of nitrous oxide from agriculture: Responses to management and climate change. *ACS Sym. Ser.* **2011**, *1072*, 343–370.
18. Wang, H.; Yang, L.; Wang, W.; Lu, J.; Yin, C. Nitrous oxide (N$_2$O) fluxes and their relationships with water-sediment characteristics in a hyper-eutrophic shallow lake, China. *J. Geophys. Res. B* **2007**, *112*, G01005. [CrossRef]

19. Hinshaw, S.E.; Dahlgren, R.A. Dissolved nitrous oxide concentrations and fluxes from the eutrophic San Joaquin River, California. *Environ. Sci. Technol.* **2013**, *47*, 1313–1322. [CrossRef]

20. Soued, C.; Giorgio, P.A.d.; Maranger, R. Nitrous oxide sinks and emissions in boreal aquatic networks in Québec. *Nat. Geosci.* **2015**, *9*, 116–120. [CrossRef]

21. Hallin, S.; Philippot, L.; Löffler, F.E.; Sanford, R.A.; Jones, C.M. Genomics and Ecology of Novel N_2O-Reducing Microorganisms. *Trends Microbiol.* **2018**, *26*, 43–55. [CrossRef] [PubMed]

22. Lai, T.; Denton, M. N_2O and N_2 emissions from denitrification respond differently to temperature and nitrogen supply. *J. Soils Sediment* **2018**, *18*, 1548–1557. [CrossRef]

23. Tomaszek, J.A.; Gardner, W.S.; Johengen, T.H. Denitrification in sediments of a Lake Erie coastal wetland. *J. Great Lakes Res.* **1997**, *23*, 403–415. [CrossRef]

24. Avrahami, S.; Liesack, W.; Conrad, R. Effects of temperature and fertilizer on activity and community structure of soil ammonia oxidizers. *Environ. Microbiol.* **2003**, *5*, 691–705. [CrossRef]

25. Jiapeng, W.; Yiguo, H.; Fengjie, G.; Yan, W.; Yehui, T.; Weizhong, Y.; Meilin, W.; Liying, B.; Jiaping, W.; Jiali, W. A rapid and high-throughput microplate spectrophotometric method for field measurement of nitrate in seawater and freshwater. *Sci. Rep.* **2016**, *6*, 20165.

26. Clough, T.J.; Buckthought, L.E.; Kelliher, F.M.; Sherlock, R.R. Diurnal fluctuations of dissolved nitrous oxide (N_2O) concentrations and estimates of N_2O emissions from a spring-fed river: Implications for IPCC methodology. *Glob. Chang. Biol.* **2007**, *13*, 1016–1027. [CrossRef]

27. Wanninkhof, R. Relationship between wind speed and gas exchange over the ocean. *J. Geophys. Res.* **1992**, *97*, 7373–7382. [CrossRef]

28. Zhao, S.; Wang, X.; Pan, H.; Wang, Y.; Zhu, G. High N_2O reduction potential by denitrification in the nearshore site of a riparian zone. *Sci. Total Environ.* **2022**, *813*, 152458. [CrossRef]

29. Vitenberg, A.G. Equilibrium model in the description of gas extraction and headspace analysis. *J. Anal. Chem.* **2002**, *58*, 6–21.

30. Hashimoto, S.; Gojo, K.; Hikota, S.; Sendai, N.; Otsuki, A. Nitrous oxide emissions from coastal waters in tokyo bay. *Mar. Environ. Res.* **1998**, *47*, 213–223. [CrossRef]

31. Yang, J.; Zhang, G.-L.; Zheng, L.-X.; Zhang, F.; Zhao, J. Seasonal variation of fluxes and distributions of dissolved methane in the North Yellow Sea. *Cont. Shelf Res.* **2010**, *30*, 187–192. [CrossRef]

32. Nils, R.-P.; Meyer, R.L.; Schmid, M.; Mike, S.M.J.; Enrich-Prast, A.; Rysgaard, S.; Revsbech, N.P. Anaerobic ammonium oxidation in an estuarine sediment. *Aquat. Microb. Ecol.* **2004**, *36*, 293–304.

33. Thamdrup, B.; Dalsgaard, T. Production of N_2O through anaerobic ammonium oxidation coupled to nitrate reduction in marine sediments. *Appl. Environ. Microbiol.* **2002**, *68*, 1312–1318. [CrossRef] [PubMed]

34. Huttunen, J.T.; Juutinen, S.; Alm, J.; Larmola, T.; Hammar, T.; Silvola, J.; Martikainen, P.J. Nitrous oxide flux to the atmosphere from the littoral zone of a boreal lake. *J. Geophys. Res. Atmos.* **2003**, *108*, D14. [CrossRef]

35. Song, A.; Liang, Y.; Zeng, X.; Yin, H.; Xu, D.; Wang, B.; Wen, S.; Li, D.; Fan, F. Substrate-driven microbial response: A novel mechanism contributes significantly to temperature sensitivity of N_2O emissions in upland arable soil. *Soil Biol. Biochem.* **2018**, *118*, 18–26. [CrossRef]

36. Poh, L.S.; Jiang, X.; Zhang, Z.; Liu, Y.; Ng, W.J.; Zhou, Y. N_2O accumulation from denitrification under different temperatures. *Appl. Microbiol. Biotechnol.* **2015**, *99*, 9215–9226. [CrossRef]

37. Maltais-Landry, G.; Maranger, R.; Brisson, J.; Chazarenc, F. Nitrogen transformations and retention in planted and artificially aerated constructed wetlands. *Water Res.* **2009**, *43*, 535–545. [CrossRef]

38. Velthuis, M.; Veraart, A.J. Temperature sensitivity of freshwater denitrification and N_2O emission—A meta-analysis. *Glob. Biogeochem. Cycles* **2022**, *36*, e2022GB007339. [CrossRef]

39. Farquharson, R.; Baldock, J. Concepts in modelling N_2O emissions from land use. *Plant Soil* **2007**, *309*, 147–167. [CrossRef]

40. Dong, L.F.; Nedwell, D.B.; Colbeck, I.; Finch, J. Nitrous oxide emission from some English and Welsh rivers and Estuaries. *Water Air Soil Poll.* **2004**, *4*, 127–134. [CrossRef]

41. Xia, Y.; Li, Y.; Ti, C.; Li, X.; Zhao, Y.; Yan, X. Is indirect N_2O emission a significant contributor to the agricultural greenhouse gas budget? A case study of a rice paddy-dominated agricultural watershed in eastern China. *Atmos. Environ.* **2013**, *77*, 943–950. [CrossRef]

42. Xiong, Z.; Xing, G.; Shen, G.; Shi, S.; Du, L. Dissolved N_2O concentrations and N_2O emissions from aquatic systems of lake and river in Taihu Lake region. *Eur. PMC* **2002**, *23*, 26–30.

43. Hartono, A.; Juliussen, O.; Svendsen, H.F. Solubility of N_2O in aqueous solution of diethylenetriamine. *J. Chem. Eng. Data* **2008**, *53*, 2696–2700. [CrossRef]

44. Weiss, R.F.; Price, B.A. Nitrous oxide solubility in water and seawater. *Mar. Chem.* **1979**, *8*, 347–359. [CrossRef]

45. Wang, Q.; Liu, S.; Tian, P. Carbon quality and soil microbial property control the latitudinal pattern in temperature sensitivity of soil microbial respiration across Chinese forest ecosystems. *Glob. Chang. Biol.* **2018**, *24*, 2841–2849. [CrossRef]

46. Liu, X.S.; Bai, J.; Sun, J.J.; Hou, R.; Zhao, Y.G. The study of denitrification rate and N_2O release rate in Shuangtaizi Estuary Wetland. *Appl. Mech. Mater.* **2014**, *665*, 416–419. [CrossRef]

47. Wang, X.; Hu, M.; Ren, H.; Li, J.; Tong, C.; Musenze, R.S. Seasonal variations of nitrous oxide fluxes and soil denitrification rates in subtropical freshwater and brackish tidal marshes of the Min River estuary. *Sci. Total Environ.* **2018**, *616–617*, 1404–1413. [CrossRef]

48. Wang, S.; Wang, W.; Zhao, S.; Wang, X.; Hefting, M.M.; Schwark, L.; Zhu, G. Anammox and denitrification separately dominate microbial N-loss in water saturated and unsaturated soils horizons of riparian zones. *Water Res.* **2019**, *162*, 139–150. [CrossRef]

49. Beaulieu, J.J.; Tank, J.L.; Hamilton, S.K.; Wollheim, W.M.; Hall, R.O., Jr.; Mulholland, P.J.; Peterson, B.J.; Ashkenas, L.R.; Cooper, L.W.; Dahm, C.N.; et al. Nitrous oxide emission from denitrification in stream and river networks. *Int. J. Biol. Sci.* **2011**, *108*, 214–219. [CrossRef]

50. Weymann, D.; Well, R.; Flessa, H.; von der Heide, C.; Deurer, M.; Meyer, K.; Konrad, C.; Walther, W. Groundwater N$_2$O emission factors of nitrate-contaminated aquifers as derived from denitrification progress and N$_2$O accumulation. *Biogeosciences* **2008**, *5*, 1215–1226. [CrossRef]

51. Hefting, M.M.; Bobbink, R.; de Caluwe, H. Nitrous oxide emission and denitrification in chronically nitrate-loaded riparian buffer zones. *J. Environ. Qual.* **2003**, *32*, 1194–1203. [CrossRef] [PubMed]

52. Saarenheimo, J.; Rissanen, A.J.; Arvola, L.; Nykanen, H.; Lehmann, M.F.; Tiirola, M. Genetic and environmental controls on nitrous oxide accumulation in lakes. *PLoS ONE.* **2015**, *10*, 0121201. [CrossRef] [PubMed]

53. Hergoualc'h, K.; Akiyama, o.; Bernoux, M.; Chirinda, N.; Prado, A.d.; Kasimir, Å.; MacDonald, J.D.; Ogle, S.M.; Regina, K.; Weerden, T.J.v.d. *2006 IPCC Guidelines for National Greenhouse Gas Inventories*; IPCC: Geneva, Switzerland, 2006.

54. Domeignoz-Horta, L.A.; Spor, A.; Bru, D.; Breuil, M.C.; Bizouard, F.; Leonard, J.; Philippot, L. The diversity of the N$_2$O reducers matters for the N$_2$O:N$_2$ denitrification end-product ratio across an annual and a perennial cropping system. *Front. Microbiol.* **2015**, *6*, 971. [CrossRef] [PubMed]

55. Yergeau, E.; Kang, S.; He, Z.; Zhou, J.; Kowalchuk, G.A. Functional microarray analysis of nitrogen and carbon cycling genes across an Antarctic latitudinal transect. *ISME J.* **2007**, *1*, 163–179. [CrossRef] [PubMed]

56. Hallin, S.; Lindgren, P.-E. PCR detection of genes encoding nitrite reductase in denitrifying bacteria. *Appl. Environ. Microbiol.* **1999**, *65*, 1652–1657. [CrossRef] [PubMed]

57. Henry, S.; Bru, D.; Stres, B.; Hallet, S.; Philippot, L. Quantitative detection of the nosZ gene, encoding nitrous oxide reductase, and comparison of the abundances of 16S rRNA, narG, nirK, and nosZ genes in soils. *Appl. Environ. Microbiol.* **2006**, *72*, 5181–5189. [CrossRef]

58. Jones, C.M.; Graf, D.R.H.; Bru, D.; Philippot, L.; Hallin, S. The unaccounted yet abundant nitrous oxide-reducing microbial community: A potential nitrous oxide sink. *ISME J.* **2013**, *7*, 417–426. [CrossRef]